NTNU

Norwegian University of
Science and Technology

The Influence of Velocity Profile on Cement Displacement Efficiency

Samwel Daud Lupyana

Petroleum Engineering
Submission date: August 2015
Supervisor: Pål Skalle, IPT

Norwegian University of Science and Technology
Department of Petroleum Engineering and Applied Geophysics

ACKNOWLEDGEMENTS

I am grateful to my supervisor Prof. Pål Skalle for his tireless guidance, support and advice. My great thanks and appreciation to StatOil Tanzania through ANTHEI scholarship scheme for financial and material support. I also extend my sincere thanks to all, who I have not mentioned here, whom without whose efforts this work would not be something substantial and complete. Lastly, I extend my heartfelt gratitude to my wife Saada and my son Lupyana Jr. for their immense love and encouragements throughout my studies and always.

SUMMARY:

The main objective of primary cement job is to provide complete isolation of the permeable zones behind the casing. This can be achieved by having an efficient cement displacement process. The challenge is always to have a displacement process which is as efficient as possible and one that cannot leave drilling mud in between the casing and cement sheath-formation interfaces. The present thesis focuses on cement displacement efficiency. It addresses the influence of the flow profiles and local turbulence due to wall roughness on the cement displacement process during laminar flow.

The study involved theoretical review and testing of the displacement model by Skalle (2014). It also involved analysis of experimental data from laboratory work by Ferizi (2014). The flow model was tested against the experimental data by plotting displacement efficiency curves and comparing them with theoretical curves for different cases of pipe roughness. The three cases, of water displacing oil were studied for water displacement in a slick pipe, in a medium rough pipe and in a very rough pipe. Three additional cases of viscous fluid displacing oil in pipes of different roughness were considered.

Theoretical analysis of the model showed that, at constant flow rate and pipe diameter, the parameter C in the model which accounts for the intensity of local velocity did not show any effect on the velocity profile. Adjustment of the original model to include the effect of local turbulence in the velocity profile. Analysis of experimental data by Ferizi (2014) showed that, the more viscous the displacing fluid was and the higher the wall roughness the higher the displacement efficiency became. Also, comparison of displacement efficiency curves from the model and experiments showed similar trends, thus indicating that the model is acceptable.

CONTENTS:

1. INTRODUCTION

Motivation

The main objective of a primary cement job is to provide complete and permanent isolation of permeable zones such as the water, oil and gas zones behind the casing. A complete cement sheath between casing and formation interfaces is also the required. The quality of the cement sheath in any cement job is important during oil and gas wells cementing. The quality of the bonding between the wall of the wellbore and the cement is highly dependent upon the sweeping efficiency of the cement slurry as it displaces the drilling mud in the annulus (Greaves 1963). The sweeping efficiency of the cement slurry depends mainly on mass balance and on the resulting displacement profile of the cement slurry, and to some extent also on the chemical compatibility between the drilling fluid and the cement slurry and type of flow characteristics of the cementing slurry (Silva et al, 1996). It is therefore purposely important to minimize the area of contact between the two during the displacement by maximizing displacement efficiency.

Displacement efficiency is the most commonly used parameter for defining the ability of a given fluid to displace another fluid. The lower the displacement efficiency the poorer the cementing job. Problems related to failures of cement jobs include cement channeling and presence of residual mud cake at the cement-formation interface. These problems result in fluid migration along micro annuli in the cemented annulus including problems related to gas migration through cement which has been a major problem in the drilling industry. Among the physical/ chemical factors which have been revealed to have an extensive influence on gas migration through cement include poor cement job as result of poor displacement. These problems therefore motivate further theoretical and experimental studies of the displacement process.

Jones and Berdine (1940) proposed effective ways to remove the mud cake which include fluid jets, scrapers or scratchers, casing reciprocation and

possibly pumping acid ahead of the displacing fluid. They also proposed to centralize the casing as a measure to minimize the problem of cement channeling after identifying, using a large scale simulator, that cement channeling was a result of casing eccentricity.

These solutions to the identified problems have a number of limitations due to the fact that they are based on laboratory, small scale approaches. The increasing complexity of the wells such as deeper wells and highly deviated wells in high temperature and high pressure environment bring new challenges. One of the key challenge in the displacement process is that, the length-to-annular-gap ratio is limited. In the laboratory, the ratio is limited of no more than 500 while in the field, it is in the order of 10^4 (Nelson, 1990). As a result of the eccentricity, this hinders the observation of axial deformation of the interface between the two fluids on a long length scale.

Goal

The aim of this project is to determine how flow profiles and pipe roughness influence cement displacement efficiency.

Approach

This work involves theoretical review of existing proposed flow and displacement models. Investigation of the displacement profile at the wall against turbulence effects during laminar flow (at $NR_e < 1800$). It also involves testing of experimental data obtained by Ferizi (2014).

2. RELEVANT KNOWLEDGE ON CEMENT DISPLACEMENT

There are several studies concerning the cement placement process which identify key factors influencing failures of primary cement jobs. Jones and Berdine (1940), using a large scale simulator, identified that poor mud displacement causes the presence of a residual mud cake at the cement-formation interface. They proposed effective ways to remove the mud cake which include fluid jets, scrapers or scratchers, casing reciprocation and possibly pumping acid ahead of the displacing fluid.

2.1. Influence of Fluid Parameters on Displacement

2.1.1. Viscosity

The viscosity of a fluid dictates the type of flow the fluid assumes. This is partly because the viscosity of a flowing fluid is related to the Reynolds number at which the fluid flows. The higher the viscosity of the fluid the lower the Reynolds number. For the case of cement as a displacing fluid, its viscosity is adjusted to fit the viscosity of the fluid that it displaces. For good sweeping, the viscosity of the cement cannot be lower than that of the drilling fluid it displaces to avoid cement fingering into the wash fluid, thus creating uneven displacement and therefore affecting the displacement profile.

2.1.2. **Density**

Density is one of the rheological parameters that affects flow profile of a displacing fluid. Gravitational effects can cause the heavier fluid to fall further down in the conduit than the lighter ones (See *Figure 1 .a*.). Likewise, lighter displacement fluid goes further up than the fluid it displaces as shown in *Figure 1 .b*. This gravitational settling effect of the heavier fluid is normally a problem when cementing horizontal wells.

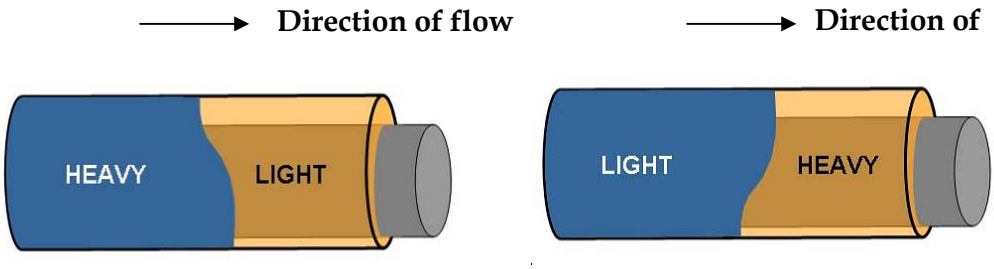

(a) (b)

Figure 1: a) Heavier displacing fluid falling to flow in the lower part of the stream. b) Lighter displacing fluid running over the heavier fluid it displaces. (Carrasco-Teja et al 2008).

It is said that usually there is a preference for displacing in turbulent regimes. If full turbulence cannot be attained, and then one of the conditions to be satisfied is for each displacing fluid to be heavier and more viscous than the fluid it displaces (Carrasco-Teja et al 2008).

2.2. Velocity Distribution in the Cement Slurry

The flow velocity distributions under different flow regimes differently influence displacement efficiency. There are basically three types of flow regimes, Laminar, plug and turbulent flow, in which a cement slurry may exist.

For the flow to be laminar or turbulent depends on a dimensionless factor called Reynolds number. This is a dimensionless quantity which is the ratio of inertial resistance to viscous resistance for a flowing fluid.

$$\mathrm{Re} = \frac{InertialForce}{ViscousForce} \tag{1}$$

At low velocities, the flow is laminar and at sufficiently high velocities, the flow is - turbulent. The velocity at which the flow turns from laminar to turbulent is called critical velocity

Studies have shown that laminar flow turns to a turbulent flow when the value of the Reynolds number given by *equation* (2) reaches a certain amount whatever the values of the average velocity v, diameter of the conduit d, fluid density ρ and fluid viscosity μ.

$$\mathrm{Re} = \frac{\rho D u_m}{\mu} \tag{2}$$

For pipe flow:

$$0 < \mathrm{Re} < 1800 \text{ Laminar flow}$$

$$1800 < \mathrm{Re} < 2300 \text{ Transition flow}$$

$$\mathrm{Re} > 2300 \text{ Turbulent flow}$$

It is also important to note that, for intermediate Reynolds numbers, the flow is transitional that is it is partly laminar and partly turbulent.

This is sometimes known as streamline flow, occurs when a fluid flows in parallel layers, with no disruption between the layers. At low velocities the fluid appears to flow in layers of varying velocity sliding past one another and without lateral mixing. There are no cross currents perpendicular to the direction of flow, nor eddies or swirls of fluids. In laminar flow the motion of the particles of fluid is very orderly with all particles moving in straight lines parallel to the walls of the conduit through which the fluid flows. This type of flow occurs when the fluid viscosity is high; velocity is below a certain value and when the conduit diameter is significantly small.

Nearly all macroscopic flows encountered in nature and in engineering practice are turbulent (Kundu et al 2012). This is the flow that occurs at higher velocities. Higher velocities lead to formation of eddies which eventually lead to lateral mixing. Velocity at a point in turbulent flow shows random fluctuations that are unpredictable in detail.

2.2.1. **Laminar Flow Regime**

The cross-sectional flow velocity under laminar flow regime is a leptokurtic distribution as shown in *figure 4a*. The velocity distribution in the laminar flow shows that, fluid near the center of the annulus has a higher axial velocity component than the fluid near the boundaries.

The velocity distribution for a fully developed laminar flow is given by the Navier-Stokes equation.

$$u = -\frac{1}{4\mu}\frac{dp}{dx}(r_o^2 - r^2) \tag{3}$$

Equation 3 is the equation of a paraboloid with maximum velocity at $r = 0$ given by the following equation.

$$u_{\max} = -\frac{1}{4\mu}\frac{dp}{dx}r_o^2 \tag{4}$$

The volumetric flow rate passing the pipe Q is given by

$$Q = -\frac{\pi r_o^4}{8\mu}\frac{dp}{dx} \tag{5}$$

And the shear stress due to the viscosity becomes

$$\tau = -\frac{1}{2}\frac{dp}{dx}r \tag{6}$$

2.2.2. **Plug Flow Regime**

The cross-sectional flow velocity under plug flow is gentle as shown in *Figure 4 b*. This type of velocity distribution favors the uniform advancing of cement slurry to displace drilling fluid (Renpu, 2011).

2.2.3. **Turbulent Flow Regime**

As the Reynolds number increases, the flow turns from laminar to turbulent through the transition region. The fluids particles start to have a fluctuating velocity in an irregular short cycle in addition to the time wise mean velocity. The fluctuating velocity behaviour is shown in *Figure 2*.

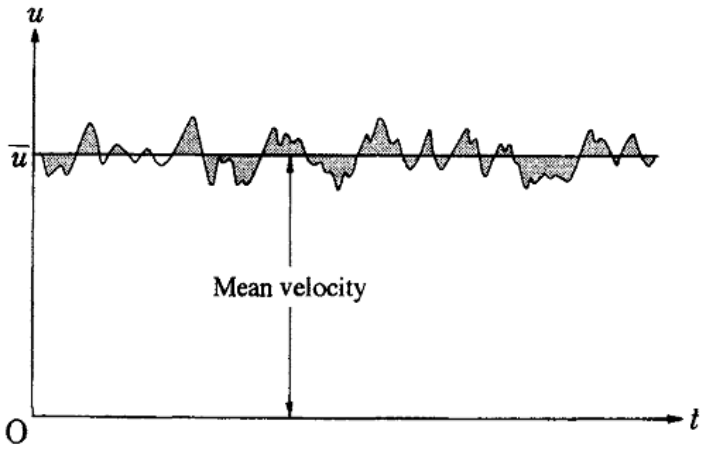

Figure 2: Turbulence (Nakayama, 1998)

For a two-dimensional flow, the velocity is given by equation (7).

$$u = \bar{u} + u' \tag{7}$$

Some scholars such as *Prandtl (1875-1953)* and *Karman (1881-1963)* managed to derive through experiments, the most useful, equation of an exponential function as the velocity distribution of a turbulent flow in a circular pipe. Eq. (8) is called Karman-Prandtl 1/7 power law and it is frequently used where n=7 because most turbulent flows are of the neighbourhood of the viscous sublayer.

$$\frac{\bar{u}}{\bar{u}_{\max}} = \left(\frac{y}{r_o}\right)^{1/n} \quad (0 \le y \le r_o) \tag{8}$$

This equation is the development from a study of the shearing stress of a turbulent flow in parallel plates which is taken as the sum of laminar flow shearing stress τ_l which is the frictional force acting between the two layers at different velocities and turbulent shearing stress τ_t where eddies mix with each other.

$$\tau = \tau_l + \tau_t \tag{9}$$

With a couple of experiments and mathematical derivation, the shearing stress of a turbulent flow was found to be given by

$$\tau = \rho\left(\nu + \nu_t\right)\frac{d\bar{u}}{dy} \tag{10}$$

Where ν_t is called the turbulent kinematic viscosity.
Prandtl (1905) made further experiments on the viscous sublayer (*see Figure 3*) came with the empirical equation shown in *equation* (11)

$$\frac{\bar{u}}{v_*} = 5.75\log\left(\frac{v_* y}{\nu}\right) + 5.5 \tag{11}$$

For each equation there should be more space, above and below
The eq. (11) is called the logarithmic velocity distribution and it is applicable up to the pipe centre from the comparison with the experimental results and to any value of Reynolds number (Yasuki Nakayama, 1998)

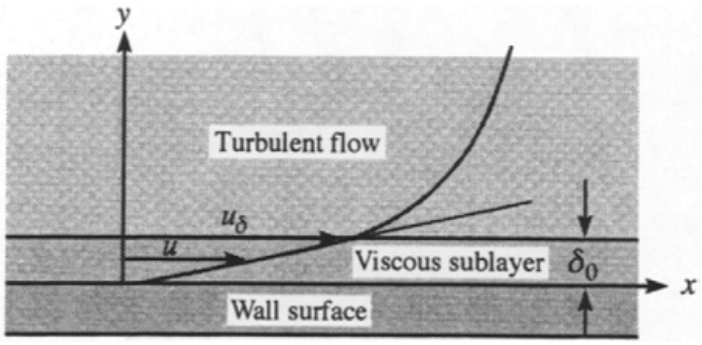

Figure 3: Viscous Sublayer (Nakayama, 1998)

Like the plug flow regime, the cross-sectional flow velocity under turbulent flow is gentle as shown in *Figure 4c*. Also, this type of velocity distribution favors the uniform advancing of cement slurry to displace drilling fluid (Renpu, 2011).

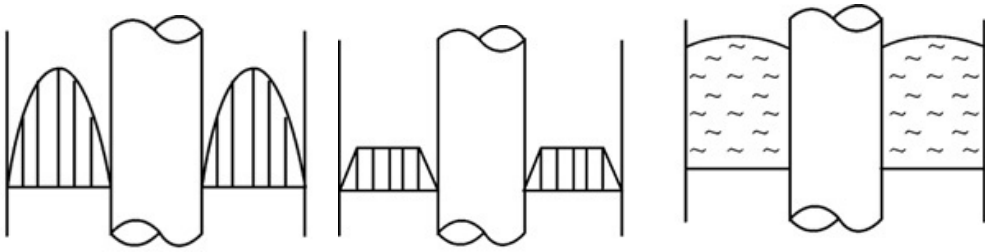

(a)Laminar flow (b) Plug flow (c) Turbulent flow

Figure 4: Flow velocity distribution under different flow regimes. (Renpu, 2011)

2.3. Displacement Efficiency

Displacement efficiency is the most commonly used parameter for defining the ability of a given fluid to displace another fluid.

2.3.1. Determining displacement efficiency

At any time, $t > 0$ displacement efficiency is defined as the fraction of the annular volume occupied by the displacing fluid, say Fluid 2 (see *Figure 5*). Mathematically, displacement efficiency, η is given by equation (12)

$$\eta = \frac{v}{Vol} \tag{12}$$

Where, v is the volume of the displacing fluid and Vol is the annular volume. The natural time scale which allows one to define the nondimensional time t^* given by equation (13) as the ratio of the flow rate Q to the annular volume Vol

$$t^* = t\frac{Q}{Vol} \tag{13}$$

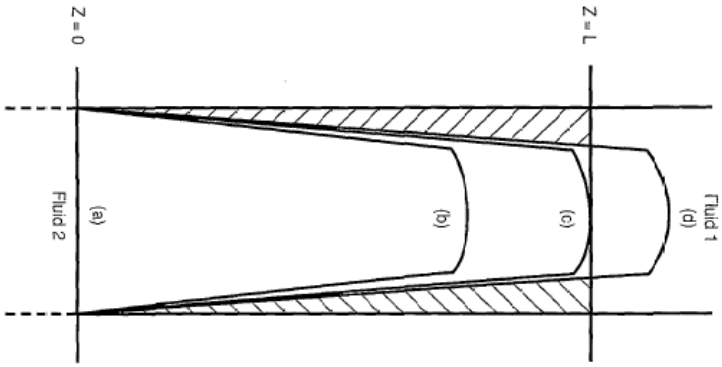

a) $t = 0$

b) $t < t_b$ (time before breakthrough)

c) $t = t_b$ (time at breakthrough) and

d) $t > t_b$ (time after breakthrough)

Figure 5: Schematic of interface profile at different times during displacement of Fluid 1 by Fluid 2 (Nelson, 1990)

Error! Reference source not found. illustrates cases that may happen during mud removal and cement placement in a wellbore.

.

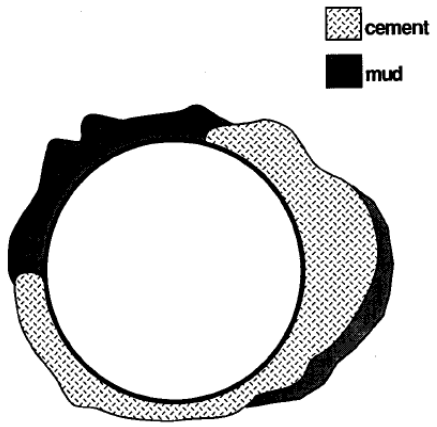

Figure 6: Illustration of a cross-section of a cemented wellbore. (After Smith,1990)

For cases like one in figure *Figure 6,* displacement efficiency can be obtained using the following equation;

$$\eta = \frac{A_{cement}}{A_{total}} \tag{14}$$

2.3.2. **Raising Displacement Efficiency of Cement**

Renpu (2011) mentions a number of measures to raise displacement efficiency. The measures include using a centralizer to reduce the eccentricity of the casing in the borehole, moving the casing during cementing, cementing under the condition of turbulent flow or plug flow, using pad fluid, adjusting drilling fluid properties before cementing and increasing contact time under a turbulent flow regime.

Using a centralizer to reduce the eccentricity of the casing

In almost all type of wells drilled, directional or horizontal wells and straight wells which are always not absolutely vertical, casing eccentricity is formed due to weight of casing. The displacement efficiency of the displacing fluid is closely related to the casing eccentricity in the borehole.

The circumferential flow velocity for a concentric annulus is even as a result of equal clearance on the whole circumference of the annulus. In an eccentric annulus, the circumferential flow velocity is uneven as compared to that in a concentric annulus due the effect of unequal clearance on the whole of the annulus. Measurements of the flow velocity distribution in an eccentric annulus has shown that, at 69% eccentricity, the flow velocity in the maximum clearance is 70 times the flow velocity in the minimum clearance (Renpu ,2011). Therefore, the eccentricity of casing in the borehole should be reduced to avoid not displacing the drilling fluid in the narrow clearance of the borehole and thus generating channel. The measure taken is to attach a centralizer to the casing string.

The conditions of flow velocity distribution in both concentric and eccentric annuli are shown in *Figure 7*.

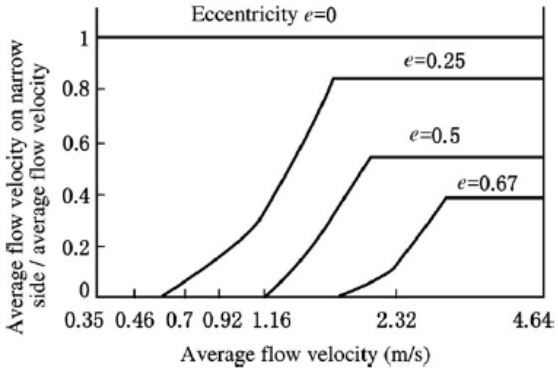

Figure 7: Flow velocity distributions in concentric and eccentric annuli (Renpu ,2011).

Moving the casing during cementing

Rotating or moving the casing up and down effectively raise displacement efficiency (Renpu, 2011).The rotating casing carries the drilling fluid held up in the narrow clearance or which flows slowly to the wider clearance. Rotating the casing may lead into excessive loading in the casing. Therefore, a speed of 10 to 20 rotations per minute is recommended (Renpu, 2011). *Figure 8* shows the measure to enhance displacement efficiency by rotating the casing.

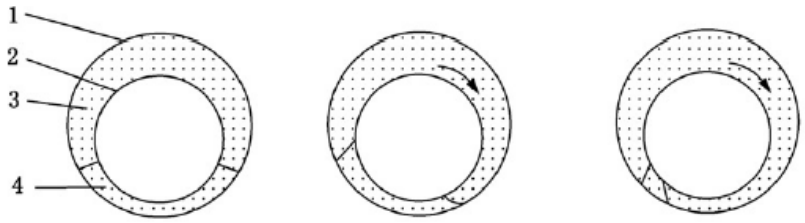

(a) Casing is static (b) Casing starts rotating (c) Drilling fluid is carried off

Figure 8: Rotating the casing to raise displacement efficiency. 1-borehole; 2-casing; 3-flowing cement slurry; 4- drilling fluid (Renpu, 2011)

Cementing under the condition of turbulent flow or plug flow

In order to achieve the best displacement, the axial velocity component as a function of the radial distance in the annulus should be as flat as possible (Vefring et al, 1997). The flatness of the velocity profile can be achieved if the cement is pumped under turbulent or plug flow. This is because the cross-sectional flow velocity distributions under turbulent and plug flow regime are relatively gentle as compared to the laminar flow regime and thus favoring higher displacement efficiency. See *Figure 4***.**

Using pad fluid

The displacement efficiency of a cement slurry, to some extent, depends on the chemical compatibility between the drilling fluid and the cement slurry and type of flow characteristics of the cementing slurry (Silva et al, 1996). It is therefore purposely important to minimize the area of contact between the two during the displacement so that to maximize displacement efficiency and obtain good quality cement sheath for a successful cementing job. To achieve this, using pad fluid is a best approach.

The pad fluid includes washing fluids for diluting the drilling fluid, washing the borehole wall and the casing wall and isolating the drilling fluid from the cement slurry and spacer fluid which is mainly for isolating the drilling fluid from the cement slurry (Renpu ,2011).

Density difference between displacement fluid and drilling fluid

The positive density difference between the displacing, pad fluid and the displaced fluid is vital requirement. This generates the buoyancy effect on the drilling fluid and therefore favors displacement (Renpu ,2011). Due to its effect of diluting the drilling fluid and washing the borehole wall and the casing wall, the washing fluid can be exempted.

2.4. Effects of Roughness on Displacement Mechanism

Roughness elements cause local flow disturbances and introduce local wall velocity fluctuations (Kandlikar, 2008). Kandlikar (2008) further states that, eddy vortex generation is a result of the instability at the boundary of the recirculating cells and the main flow. In case of a single roughness structure, eddies are introduced downstream and relaminarization occurs beyond a certain distance as shown in *Figure 9*. Relaminarization depends on the Reynolds number and the height and shape of the roughness structure (Kandlikar, 2008).

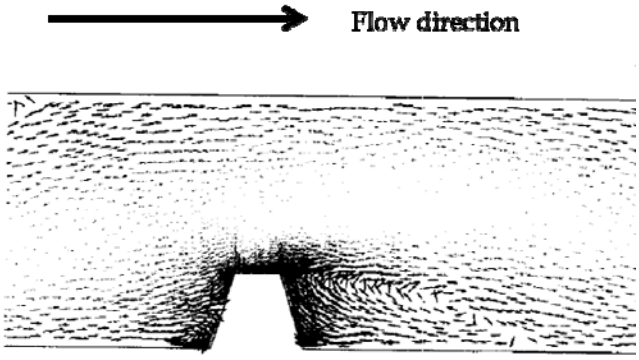

Figure 9: Flow structure following a single roughness element. Eddies are seen to be created downstream just after the roughness structure and a distance further down relaminarization occurs. (Kandlikar, 2008)

For closely spaced roughness elements, the recirculation cells are formed between the roughness structures as shown in *Figure 10*. Kandlikar *et al* (2005) in there experiment, using saw-tooth roughness structures in rectangular flow

channels, used the effective diameter of the pipe which they called constricted flow diameter, d_{cf} defined by eq. (15)

$$d_{cf} = d - 2\varepsilon \tag{15}$$

where d is the internal diameter of the conduit and ε is the size of the roughness element as seen in *Figure 11.* The velocity is high downstream the roughness structures and low just above the edges where the flow is purely laminar.

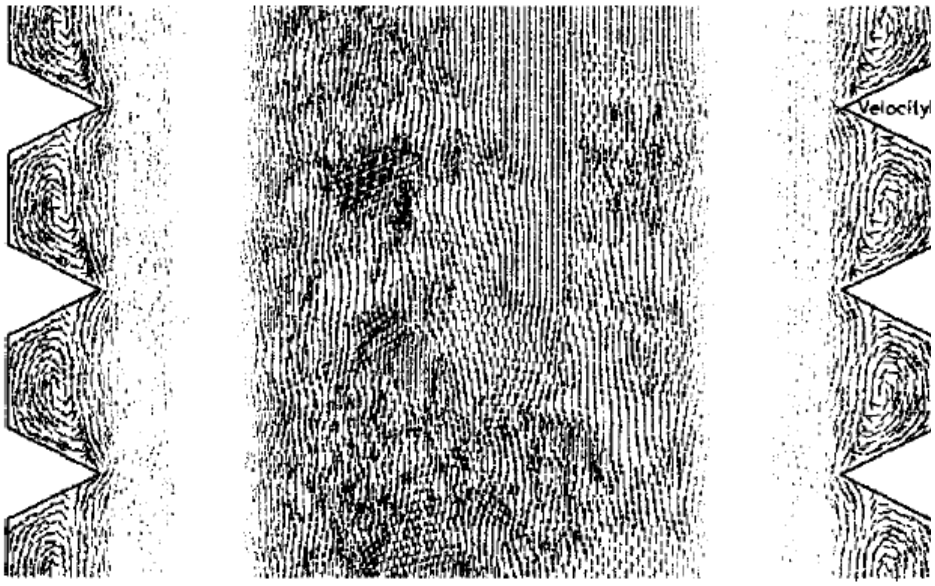

Figure 10: Flow structure for closely spaced 2-D roughness elements. (Kandlikar, 2008)

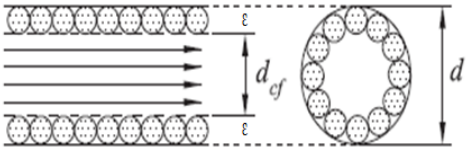

Figure 11: Flow pattern in a rough pipe (Huang et al, 2013).

Skalle (2014) proposed a theoretical model which can be used in cases where there is local turbulence. The model shows a velocity profile, given by equation (16), that includes the turbulent flow close to the wall.

$$u(r) = u_{local} + u_{\max}\left(C - \frac{r^2}{r_o^2}\right) \tag{16}$$

Skalle (2014) states that the two velocities, the turbulent velocity due to roughness elements, u_{local} and the laminar velocity in the main stream, are the two possibly hypothetical velocity profiles as seen in *Figure 12*. The magnitude of u_{local} is dictated by the surface roughness and Reynolds number.

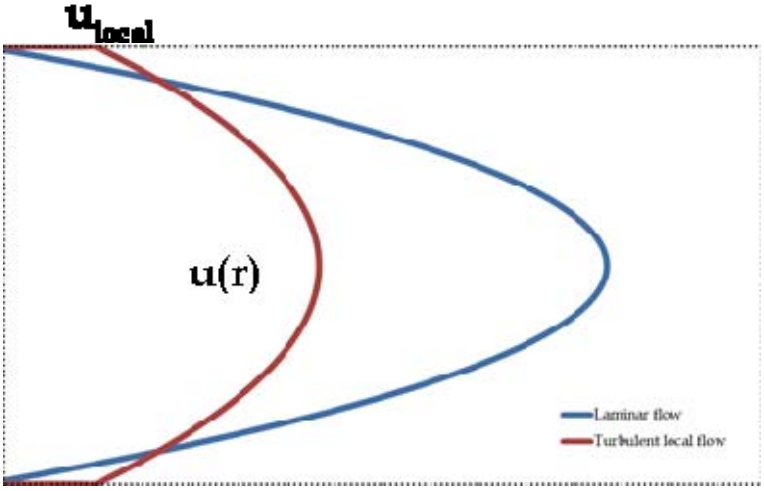

Figure 12: Two competing hypothesises of flow profiles development: One is turbulent due to roughness structures at the wall and the other is purely laminar.

To conserve the mass, while pumping at a certain volumetric flow rate, say q, the two velocity profiles in *Figure 12* need to be defined by the same flow rate such that, if q_1 and q_2 are the respective volumetric flow rates for the two velocity profiles, then; $q_1 = q_2 = q$ .This is why the two velocity can be used to estimate the unknown u_{local}.

The displaced volume collected after breakthrough is probably different in turbulent profile compared to purely laminar profile due to the difference in the volumetric shape of the two flow profiles despite arising from the same flow rate.

Skalle (2014) further suggests that, the position of the displacement front is a parabolic profile function of the velocity, given by eq. (16), and time, t of displacement as shown in equation (17)

$$l(\mathrm{r},t) = u(r)t \tag{17}$$

the travel length of the its center-flow is given by equation (18)

$$l_{\max}(t) = u_{\max}t \ \ (\text{at } r = 0\ ) \tag{18}$$

and the coefficient C which accounts for the intensity of the local velocity is given by equation (19)

$$C = 1 - \frac{u_{local}}{u_{\max}} \tag{19}$$

3. DEVELOPING THE SELECTED MODEL.

3.1. Models by Skalle (2014)

For the further investigation, velocity and displacement profile models by Skalle (2014) are selected (see eq. (20), (21) and (22)). The models are simple because they involve the study of 2-D cases in both the flow pattern and the roughness structures. In nature, the roughness elements are generally 3-D but the 2-D case can easily be deployed in both experimental and numerical investigations.

$$l(\mathrm{r},t) = u(r) * t \tag{20}$$

$$u(r) = u_{local} + u_{\max}\left(C - \frac{r^2}{r_o^2}\right) \tag{21}$$

$$C = 1 - \frac{u_{local}}{u_{\max}} \tag{22}$$

Mathematical determination of local velocity, u_{local} by solving eq. (21) by Skalle (2014) requires solving for C from the eq. (21);

$$\Rightarrow C = \frac{u(r) - u_{local}}{u_{\max}} + \frac{r^2}{r_o^2} \tag{23}$$

$$\Rightarrow C = \frac{u(r)}{u_{\max}} + \frac{r^2}{r_o^2} - \frac{u_{local}}{u_{\max}} \tag{24}$$

From Navier-Stokes equation,

$$u(r) = u_{\max}\left(1 - \frac{r^2}{r_o^2}\right) \tag{25}$$

$$\Rightarrow \frac{u(r)}{u_{\max}} = \left(1 - \frac{r^2}{r_o^2}\right) \tag{26}$$

Substituting $\frac{u(r)}{u_{\max}}$ into eq. (24); eq. (22) that determines the intensity of the local velocity as suggested by Skalle (2014) is obtained. It follows that

$$u_{local} = (1 - C)u_{\max} \tag{27}$$

The expression of the frontal radius can be obtained from eq. (20) , (21) and (22) and is given by equation (28).

$$r(l,t) = r_o\sqrt{1 - \frac{l(r,t)}{u_{\max}(\mathrm{t}) * t}} \tag{28}$$

3.2. Improving the model by Skalle (2014)

Mathematical adjustment of the displacement model given in eq. (21) by Skalle (2014) is required because initial simulation of the eq. shows that it does not take in the effects of the coefficient C which accounts for the wall roughness and therefore shows the intensity of the local velocity in the model.

From Skalle (2014) theoretical models given in eq. (21) and (22), substituting eq. (22)into eq. (21)

$$\Rightarrow u(r) = u_{local} + u_{\max}\left(1 - \frac{u_{local}}{u_{\max}} - \frac{r^2}{r_o^2}\right) \tag{29}$$

and it follows therefore,

$$u(r) = u_{\max}\left(1 - \frac{r^2}{r_o^2}\right) \tag{30}$$

Eq. (30) does not include the local velocity due to local turbulence as a result of wall roughness. (See *Table 1)*

Table 1: Table showing velocities at distances from the centre of the pipe, different values of parameter C in equation (21) at constant flow rate of 0.000007065m³/s.

C	0	0.2	0.4	0.6	1
r	Velocity, u(r)				
0	0.18	0.18	0.18	0.18	0.18
0.00001	0.17999928	0.17999928	0.17999928	0.17999928	0.17999928
0.00002	0.17999712	0.17999712	0.17999712	0.17999712	0.17999712
0.00003	0.17999352	0.17999352	0.17999352	0.17999352	0.17999352
0.00004	0.17998848	0.17998848	0.17998848	0.17998848	0.17998848
0.00005	0.17998200	0.17998200	0.17998200	0.17998200	0.17998200
0.00006	0.17997408	0.17997408	0.17997408	0.17997408	0.17997408
0.00007	0.17996472	0.17996472	0.17996472	0.17996472	0.17996472
0.00008	0.17995392	0.17995392	0.17995392	0.17995392	0.17995392
0.00009	0.17994168	0.17994168	0.17994168	0.17994168	0.17994168
0.00010	0.17992800	0.17992800	0.17992800	0.17992800	0.17992800

To include the effect of wall roughness, the adjustment to the model by Skalle (2014) is made and $u(r)$ in eq. (21) is given by the following equation;

$$u(r) = u_{local} + u_{\max}\left(1 - \frac{r^2}{r_o^2}\right) \tag{31}$$

and the assumption is the local velocity is a fraction of the centerline velocity during laminar flow.

$$i.e \;\; u_{local} = bu_{\max} \tag{32}$$

where b is in the range $0 \le b \le 1$ and it is assumed $b = 0$ for a smooth pipe and $b = 1$ for a completely rough pipe. Substituting eq. (32) into (31) it follows that;

$$u(r) = u_{\max}\left[(1+b) - \frac{r^2}{r_o^2}\right] \tag{33}$$

Putting $C = (1+b)$ into eq. (33), it therefore follows that,

$$u(r) = u_{\max}\left(C - \frac{r^2}{r_o^2}\right) \tag{34}$$

In eq. (34), C takes the range $1 \le C \le 2$ whereby it is assumed $C = 1$ for a smooth pipe and $C = 2$ for a completely rough pipe.

The adjusted expression of the frontal radius can be obtained from eq. (20) , and (34) as is given by equation (35).

$$r(l,t) = r_o\sqrt{C - \frac{l(r,t)}{u_{\max}(\mathrm{t}) * t}} \tag{35}$$

3.3. Determination of theoretical displacing fluid volumes in pipe

Considering the displacement profile volume as is made of very small disc shaped volume elements of equal thicknesses dl as shown in the following figure,

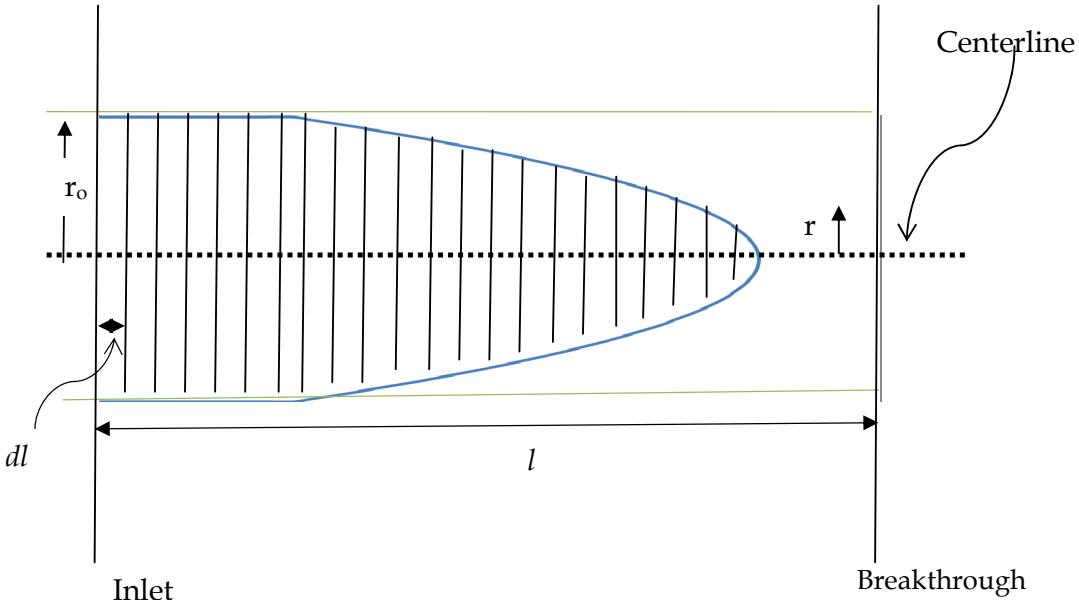

Volume of a single disc is given as

$$dV = \Pi r^2 dl \tag{36}$$

$$\Rightarrow dV = \Pi \left[f(l) \right]^2 dl \tag{37}$$

But $f(l) = \mathrm{r}$ the front radius which is a function of the front position, l .

$$\Rightarrow [f(l)]^2 = r^2 = r_o^2 \left[C - \frac{l(t)}{l_{\max}(t)} \right] \tag{38}$$

Substituting (38) into (36) , it follows that;

$$dV = \Pi r_o^2 \left[C - \frac{l(t)}{l_{\max}(t)} \right] dl \tag{39}$$

To obtain the total volume of the displacing fluid in pipe, V_{pipe_df} an integral sum of the small volume elements is taken as follows;

$$V_{pipe\_df} = \Pi r_o^2 \int_0^{l(t)} \left[C - \frac{l(t)}{l_{\max}(t)} \right] dl \tag{40}$$

and therefore instantaneous volume of the displacing fluid in the pipe is given by equation (41).

$$V_{pipe\_df} = \Pi r_o^2 \left[Cl(t) - \frac{l^2(t)}{2l_{\max}(t)} \right] \tag{41}$$

3.4. Determining theoretical displacement efficiency

During theoretical investigation, the displacement efficiency, η is calculated using the following equation.

$$\eta = \frac{V_{pipe\_disdf}}{V_{pipe\_total}} \tag{42}$$

where by, V_{pipe_disdf} and V_{pipe_total} are respectively the volumes of the displaced fluid in the pipe section and the total volume of the pipe section between the inlet and the point of breakthrough.

Figure 13 shows an example of the displacement profile and the area covered by the displacing fluid in 2D.

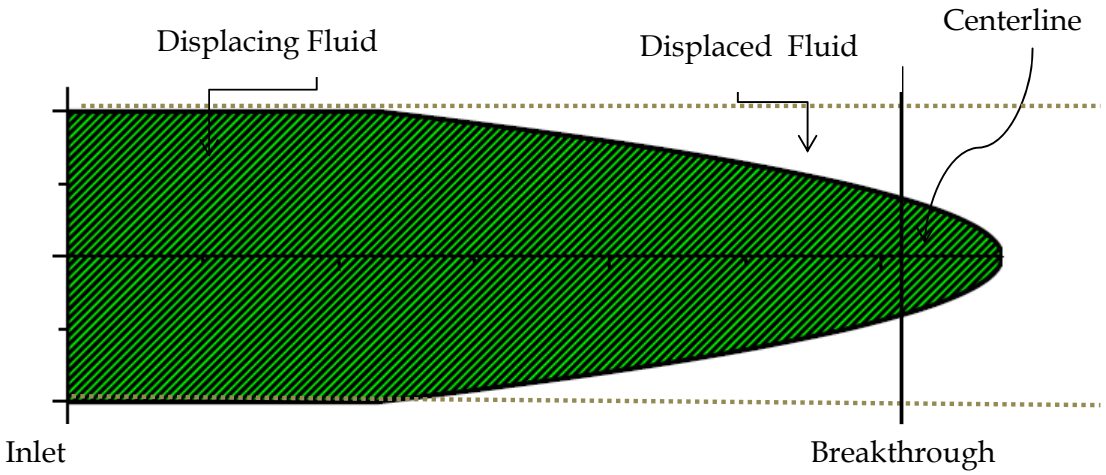

Figure 13: Displacement profile

The volume of the displacing fluid in the pipe during displacement is given by equation (41). It is therefore possible to obtain the volume of the displaced fluid remaining in the pipe section as follows;

$$V_{pipe\_disdf} = V_{pipe\_total} - V_{pipe\_df} \tag{43}$$

The volume of the displacing fluid pumped into the pipe section during displacement time, t is given in eq. (41).

After obtaining the volume of the displacing fluid in the pipe, it is then possible to find the displacement efficiency given by eq. (42). Obtaining the frontal position of the flow at a given time is therefore a prerequisite for determining the displacement efficiency.

For simplicity, the volume of the displacing fluid replacing the displaced fluid is equal to that of the displaced fluid after breakthrough (referring a case of

conservation of mass). The flow time is obtained from the total volume measured after breakthrough and the measured flow rate such that;

$$t = \frac{V_{produced\_total}}{q_{pump}} \tag{44}$$

This is the time taken for a given volume of the displaced fluid to be replaced by the displacing fluid. Using this time in eq. (20), frontal positions along the velocity profile can be obtained.

3.5. Simulation of the adjusted selected model

The simulation of the adjusted displacement models by Skalle (2014) is presented here to compare if the model approximates to the experimental results.

The observations I present here are under the assumptions that the displacing fluid being considered is water with the following properties; Density of water is 1000 kg/m^3 and the dynamic viscosity is 1 cP. The water flows in a pipe of inside diameter 0.01 m and a length of 6 m so as to have the same properties as the pipe that was used by Ferizi (2014) in her experimental work. The maximum adopted flow rate should give the Reynolds number of at most 1800.

In the simulations, eq. (34) is used to determine the radial velocities at different points along the flow profile. These velocities are used in eq.(20) to obtain their respective front positions. The velocity values are basically the velocities of individual layers in the main stream thus the front positions are particularly front positions for those individual layers which are along $0 \le r \le r_o$.

With the measured total volume displaced, displaced oil volume and flow rate, the flow time is obtained using eq. (44). Using the radial velocities at different radial position and eq.(20) in the simulation, then the individual

front positions can be obtained. Finally, the displacement efficient is obtained using the relation given in eq. (42).

Simulation of the selected flow and displacement models given in equations (20), (34) and (35) was done using MS Excel under the assumptions above. The simulation results are used to plot displacement efficiency curves of which are drawn using the displacement efficiency in percentage against the number of pipe volumes displaced in wholes of one pipe volume. The following equation is used in determining the number of pipe volumes displaced after given flow time, t .

$$N_v = \frac{V_{produced\_total}}{V_{pipe\_total}} \tag{45}$$

4. PRESENTATION OF EXPERIMENTAL DATA.

4.1. Experimental Set Up and Test Procedures

Experimental set up and data collection procedures by Ferizi (2014) are presented here.

4.1.1. Experimental Set Up

Pipes of length 6.0 m and internal diameter of 1.0 cm were used in her set up as seen in *Figure 14.* The inside of the pipes were introduced with three types of roughness namely; smooth, medium roughness and very rough. The pipe was laid on a table at an angle of 20° so that to make it full during filling up. The pipes with different roughness were then used for displacement experiments at different flow rates. The displaced volume was measured through a measuring cylinder as seen in *Figure 14* which illustrates the experimental set up by Ferizi (2014).

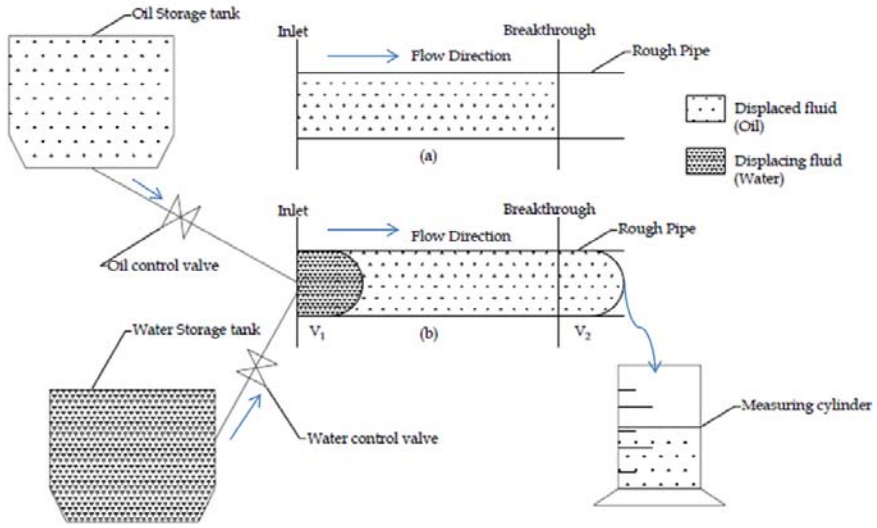

Figure 14: Illustration of experimental set up by Ferizi (2014). a) A pipe is filled with fluid to be displaced (Oil) and this pipe is tilted at an angle of 20° from horizontal to make it full. b) Displacement process experimented with the displacing fluid (water) being introduced to the pipe from a pressure tank in an elevation higher than that of the pipe.

When both the displacing (water for this case) and the displaced fluid (oil) were collected in the measuring cylinder, since the two are immiscible, the measurements were taken from the point of separation of the two fluids. Oil is lighter than water thus covered the top portion of the volume in the measuring cylinder.

4.1.2. Test procedures

In her experimental work, Ferizi (2014) used the following test procedures to perform each test;

i. Filled the test pipe with oil which acted as the fluid to be displaced by opening the flow valve between oil tank and pipes. The pressure head difference between the tank and the pipes was adequate to flush any residual displacing fluid (water or viscous fluid).
ii. Pressure in the tank containing the displacing fluid (water) was adjusted to give a desired flow rate.
iii. Adjusted pressure control valve to a set flow rate.
iv. Turned on the gate valve to allow flow from pressure tank to pipes.
v. Stop watch was turned on as the gate valve was turned on.
vi. When the cylinder was filled up to desired amounts of pipe volumes, the gate valve from the pressure tank to the pipe was closed and stop watch was stopped at the same instant.
vii. Readings of actual amount of displaced volume was taken. (see *Figure 15* and eq. (46)).
viii. After complete separation of the fluids in the cylinder, Readings of amount of displaced oil is also taken (Also see *Figure 15* , the top part of the volume in the measuring cylinder). The precision of the readings of displaced volume was accurate down to 0.05 deciliters.
ix. The ratio of the total displaced volume to the recorded flow time was taken to give the flow rate. Flow rate was used to find the Reynolds

number inside the pipe for each measurement, allowing us to know if the flow was turbulent, laminar or transient.

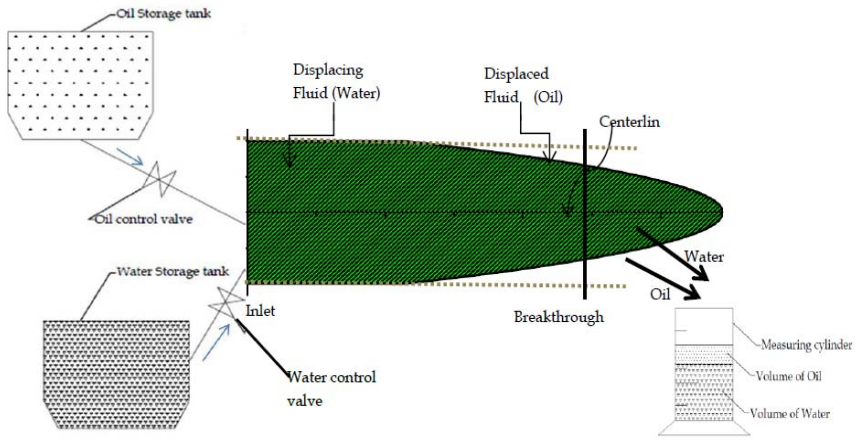

Figure 15: Illustration of experimental set up by Ferizi (2014). The readings taken from the measuring cylinder included $V_{produced\_total}$ which is the total volume collected in the measuring cylinder (volume of oil and volume of water)

Note:

The reading taken during procedure vii) in the test procedures is given by eq. (46).

$$V_{produced\_total} = V_{produced\_oil} + V_{produced\_water} \tag{46}$$

where by $V_{produced\_oil}$ and $V_{produced\_water}$ are respectively volumes of produced oil and water in the measuring cylinder after complete separation.

The displacement time, t recorded in procedure vi) was used to calculate the flow rate of the displacement process such that;

$$q_{pump} = \frac{V_{produced\_total}}{t} \tag{47}$$

4.2. Test Results.

The test results for each displacement case experimented were presented in tables and used to draw displacement efficiency curves for analysis. See

Table **2** as a sample table.

Table 2: Sample experimental data for the case of water displacement in a medium rough pipe (source: Ferizi, 2014)

Displaced Volume [m^3]	Flow Rate, Q [m^3/s]	Reynolds Number, NRe	Percentage Oil Displaced [%]	Displaced Units
0.00034	0.000001	162	72	0.72
0.00047	0.000003	384	100	1
0.00047	0.000003	392	100	1
0.00157	0.000003	398	100	3.32
0.0003	0.000005	729	64	0.64
0.00066	0.000006	832	100	1.4
0.00128	0.000009	1353	92	2.72
0.00034	0.00001	1475	72	0.72
0.00811	0.000011	1613	100	17.22
0.00828	0.000011	1632	100	1758
0.00615	0.000012	1678	100	13.05
0.00415	0.000012	1732	96	8.81
0.00119	0.000012	1736	96	2.52
0.0003	0.000012	1761	60	0.64

Again, *Figure 16* is a sample presentation of displacement efficiency curves by Ferizi (2014) which shows comparison on effect of pipe roughness on displacement efficiency.

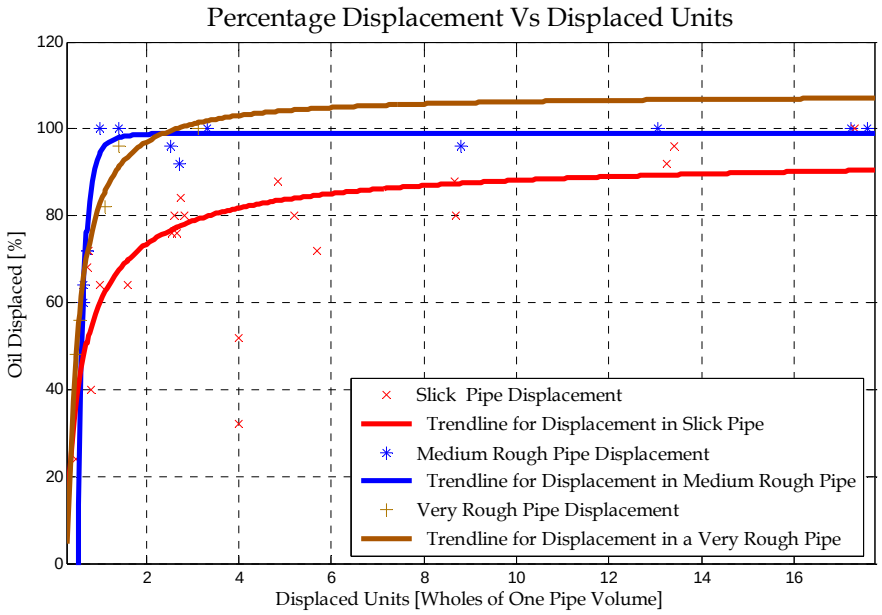

Figure 16: Percentage displacement for pipes of different internal roughness. Reynolds number less than 1800. (Drawn using data from Ferizi (2014))

The displacement efficiency values in percentage where obtained by taking the ratio of the volume of produced oil over the total volume of the pipe section (The 6 m pipe used in the experiment). The ratio is presented in eq. (48).

$$\eta_{lab} = \frac{V_{produced\_oil}}{V_{pipe\_total}} x100 \tag{48}$$

and the displaced units which were taken as wholes of one pipe volume were obtained using eq. (49).

$$N_v = \frac{V_{produced\_total}}{V_{pipe\_total}} \tag{49}$$

The test results presented by Ferizi (2014) in *Figure 16* show that displacement efficiency increases as the pipe roughness increases. A very rough pipe has higher displacement efficiency than a medium rough pipe and likewise a medium rough pipe has higher displacement efficiency than a slick pipe. This trend of increase in displacement efficiency seems to be a result of the local turbulence introduced by the roughness elements at the wall of the pipe.

5. RESULTS AND DISCUSSION

5.1. Results

5.1.1. Results from simulation of the adjusted selected model

Results of the simulation presented in section 3.5 for the case of water displacement for pipes of three different internal roughness are presented. *Figure 17* shows the comparison for three different values of the coefficient C, including when $C=1.0$, $C=1.5$ and $C=2.0$ to respectively represent experimental case for slick pipe, medium rough pipe and very rough pipe. In eq. (34), the parameter C is in the range $1 \le C \le 2$ whereby it is assumed that $C=1$ for a smooth pipe and $C=2$ for a completely rough pipe.

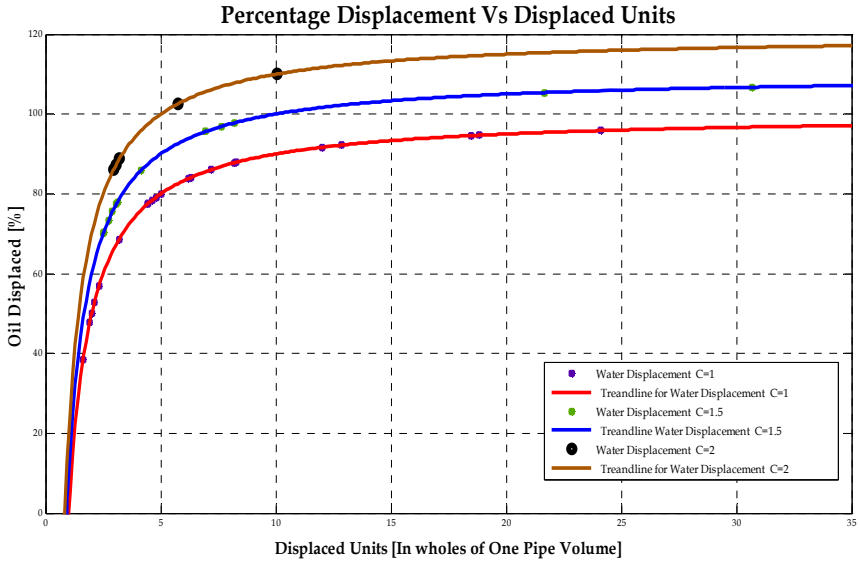

Figure 17: Comparison of water displacement cases for different pipe roughness by changing C values. (Drawn using theoretical model and the experimental flow rates)

Table 3 shows theoretical values obtained after simulation of eq.(34).

Table 3: Theoretical values of radial velocity obtained from simulation of the adjusted displacement model

C	1	1.1	1.4	1.5	1.6	1.9	2
r[m]	U(r) [m/s]						
0	0.4076	0.4484	0.5707	0.6115	0.6522	0.7745	0.8153
0.0001	0.4075	0.4482	0.5705	0.6113	0.6521	0.7744	0.8151
0.0002	0.4070	0.4478	0.5700	0.6108	0.6516	0.7739	0.8146
0.0003	0.4062	0.4469	0.5692	0.6100	0.6508	0.7731	0.8138
0.0004	0.4050	0.4458	0.5681	0.6089	0.6496	0.7719	0.8127
0.0005	0.4036	0.4443	0.5666	0.6074	0.6482	0.7704	0.8112
0.0006	0.4018	0.4425	0.5648	0.6056	0.6464	0.7687	0.8094
0.0007	0.3997	0.4404	0.5627	0.6035	0.6442	0.7665	0.8073
0.0008	0.3972	0.4380	0.5603	0.6010	0.6418	0.7641	0.8049
0.0009	0.3944	0.4352	0.5575	0.5983	0.6390	0.7613	0.8021
0.001	0.3913	0.4321	0.5544	0.5952	0.6359	0.7582	0.7990
0.0011	0.3879	0.4287	0.5510	0.5917	0.6325	0.7548	0.7956

5.1.2. Comparison between experimental data and model data

The following cases are presented.

i. Comparison of model data and experimental data for water displacement in a slick pipe

Figure 15 shows comparison between theoretical and experimental water displacement cases in a slick pipe. The trend line curves for the two cases assume the same nature.

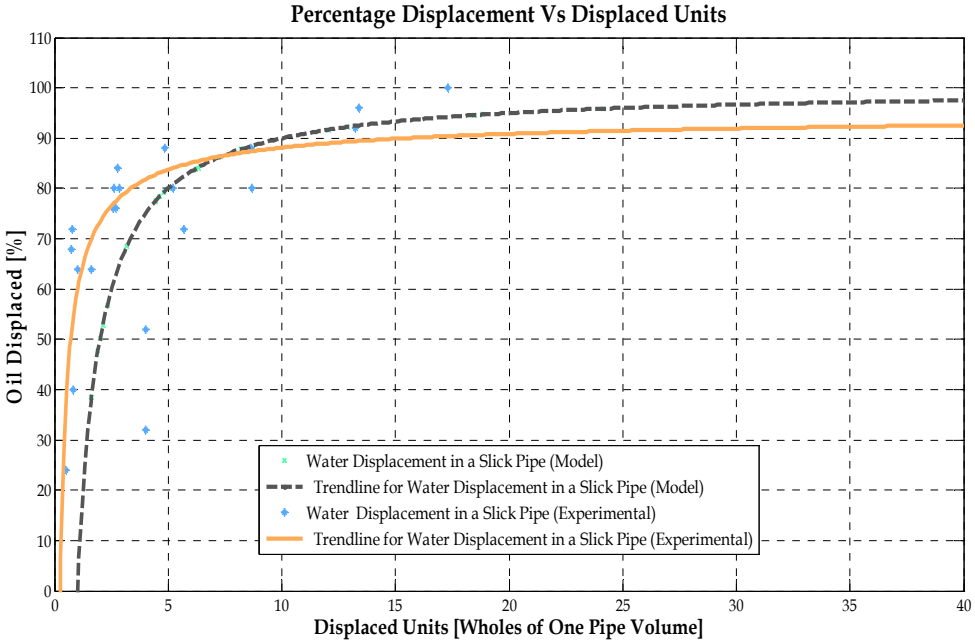

Figure 18: Comparison between theoretical and experimental water displacement in a slick pipe.

ii. Comparison of model data and experimental data for water displacement in a medium rough pipe

Figure 16 shows comparison between theoretical and experimental water displacement cases in a medium rough pipe. The trend line curves for the two cases assume the same nature.

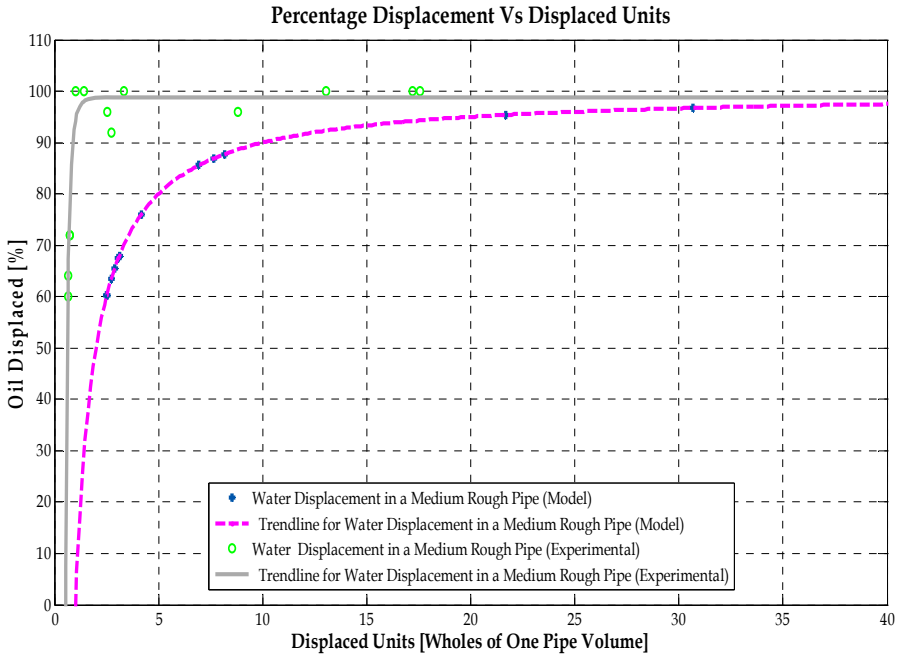

Figure 19: Comparison between theoretical and experimental water displacement in a medium rough pipe.

iii. Comparison of model data and experimental data for water displacement in a very rough pipe

Figure 17 shows comparison between theoretical and experimental water displacement cases in a very rough pipe. The trend line curves for the two cases assume the same nature.

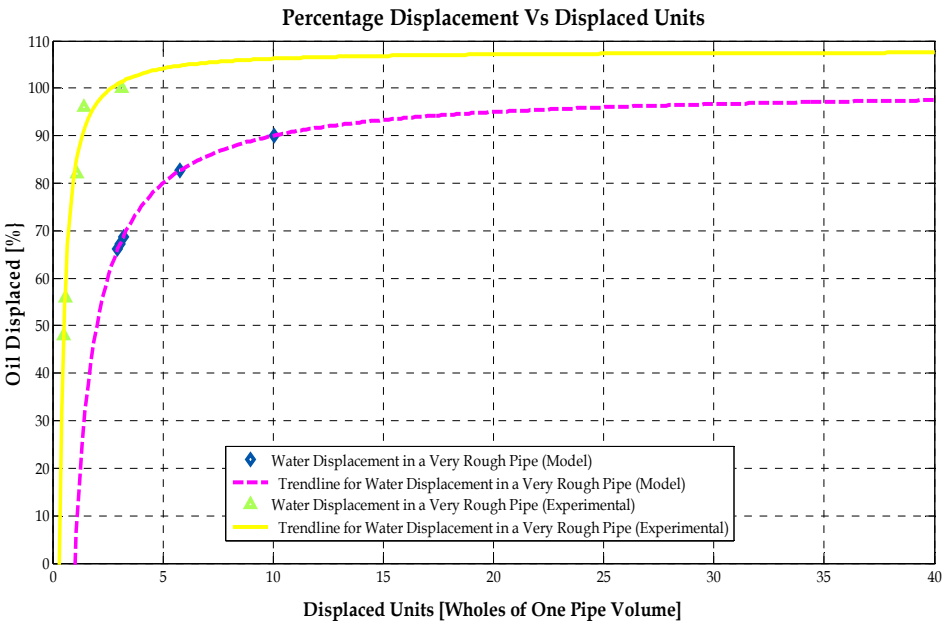

Figure 20: Comparison between theoretical and experimental water displacement in a very rough pipe.

5.1.3. Determination of the local velocity

The local velocity is determined by solving results from the adjusted model, given by eq. (34), with respect to u_{local} . Determining u_{local} values using the original model is ineffective, the reason being failure of the model to take into account the effect of roughness taken in by the parameter C in the model. *Table 4* shows u_{local} values obtained by solving the adjusted model.

Table 4: Determined values of local velocity, u_{local} obtained by solving the adjusted model

Reynolds Number, Nre			Local Velocity, u_{local} [m/s]					
			Slick		Medium Rough		Very Rough	
Slick	Medium Rough	Very Rough	C=1.5	C=2	C=1.5	C=2	C=1.5	C=2
645	162	76	0.0574	0.1148	0.0144	0.02884	0.00676	0.0135
828	384	160	0.0737	0.1474	0.0342	0.06835	0.01424	0.0285
854	392	194	0.076	0.152	0.0349	0.06978	0.01727	0.0345
901	398	375	0.0802	0.1604	0.0354	0.07084	0.03338	0.0668
1009	729	439	0.0898	0.1796	0.0649	0.12976	0.03907	0.0781
1038	832		0.0924	0.1848	0.0741	0.1481		
1054	1353		0.0938	0.1876	0.1204	0.24083		
1065	1475		0.0948	0.1896	0.1313	0.26255		
1162	1613		0.1034	0.2068	0.1436	0.28711		
1188	1632		0.1057	0.2115	0.1453	0.2905		
1233	1678		0.1097	0.2195	0.1493	0.29868		
1258	1732		0.112	0.2239	0.1542	0.3083		
1276	1736		0.1136	0.2271	0.1545	0.30901		
1285	1761		0.1144	0.2287	0.1567	0.31346		
1461			0.13	0.2601				
1516			0.1349	0.2699				
1522			0.1355	0.2709				
1629			0.145	0.29				
1642			0.1461	0.2923				
1685			0.15	0.2999				
1747			0.1555	0.311				

Figure 21 shows the effect of changing the parameter C in determining u_{local}, using the adjusted displacement model, at constant flow rates. As C increases (indication of increase in roughness), the local velocity increases as well.

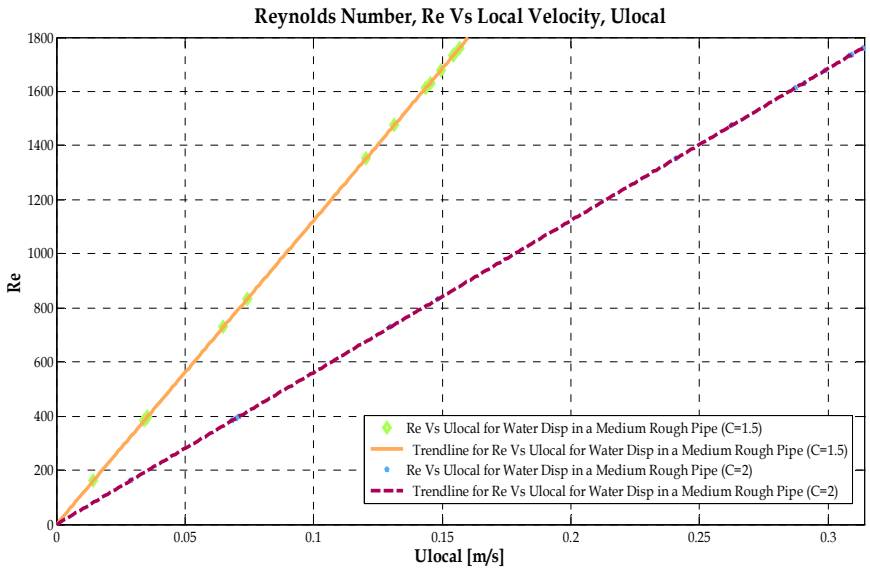

Figure 21: Comparison between theoretical and experimental viscous displacement in a medium rough pipe.

5.2. Discussion.

Both theoretical analysis of the displacement models and the experimental data show that a number of parameters influence displacement efficiency. It is observed that, a flatter velocity profile promotes a higher displacement efficiency. It is also seen that, a flatter displacement profile is a result of wall roughness due to the fact that, roughness at the wall creates local turbulence along the wall which in turn produce flatter displacement profiles and hence higher displacement efficiency.

6. ASSESSMENT OF THE WORK

Theoretical analysis of the model and the experimental data has helped identifying the usefulness and shortcoming of the model and experimental work by Sera. The information is helpful for others who can go some further steps ahead in, for example, experimentally quantifying for the parameter C in the model in equations (16) and (19).

6.1. Quality of the Model

The model given in equation (16) is simple as it fails to include the effects of surface roughness directly. As seen in *Table 1* above, at a constant flow rate and pipe diameter, different values of the parameter C in the model give the same values of velocity at a given radial distance from the pipe wall. The parameter C in the model, in real flow conditions, is dictated by the Reynolds number and surface roughness. Changing the value of the parameter C at this situation theoretically, would mean accounting for the effect of surface roughness. In present studies it has shown no effect. Through better procedures and improved experiments, the model can be improved to effectively account for the effect of surface roughness.

6.2. Quality of the Laboratory Data

It is difficult to compare the theoretical work with the experimental data from lab as taken by Sera Ferizi for the fulfilment of her thesis work, Cement Displacement Efficiency, NTNU, June 2014. The organization of data is not good. This brings difficulties for someone else to work with the data. As an example see

Table **5** which is adopted from appendix B4 in Sera's work.

Table 5: Sample laboratory data (adopted from Ferizi, 2014)

Displaced Volume [m^3]	Flow Rate, q [m^3/s]	Reynolds Number, NRe	Volume of Oil [m^3]	Percentage Oil Displaced [%]	Number of Displaced Volumes
0.00052	0.000001	76	0.00039	82	1.1
0.00026	0.000001	160	0.00026	56	0.56
0.00023	0.000001	194	0.00023	48	0.48
0.00147	0.000003	375	0.00047	100	3.12
0.00066	0.000003	439	0.00045	96	1.4

Table **5** shows that at the same pipe diameter and flow rate of 0.00001m^3/s, the flow Reynolds numbers varies. This is also observed at the flow rate of 0.000003m^3/s. Theoretically, from equation (2), if the fluid and the pipe properties are the same, the Reynolds number is constant at constant flow rate and pipe diameter. It is again difficult to say if the quality of the data was poor or just the way they were organized to serve the purpose. In short, the data have a lot of uncertainties which need to be worked on.

Again the data had to be taken to allow sensitivity analysis of the model. For instance, experiments would have to be done while changing one parameter at a time say keep constant flow rates and fluid properties for pipes of different roughness. And repeating the experiments at changing fluid properties.

6.3. Improving the Work

To improve the work, further experiments have to be conducted to study the effects of surface roughness and its influence on fluid displacement and velocity profiles. It has also to be studied how surface roughness influences the Reynolds number because testing of the model has only touched parts related to changing flow velocity and size of the pipe.

It can further be improved by studying the effects of flow geometry. At what change of flow geometry does the flow, at any particularly low flow rate, turn from laminar to eddies.

7. CONCLUSION

From analysis and the results obtained, it seems there is still much effort needed to experimentally and theoretical study the cement displacement process. Present work indicates that both the theoretical and experimental work is needed. It also points out that, the displacement profile is largely influencing the cement displacement efficiency.

Achievements in present work

- Displacement efficiency was theoretical modelled and fitted to experimental data.
- It was discovered that the local turbulence due to roughness along the wall introduces a local velocity whose magnitude depends on the size of the roughness elements.

Limitations

- The experiments need to be performed with higher accuracy including recording and precise reporting of all relevant information such as time of displacement, produced volumes of both displacing and displaced fluids etc.
- The model should also include the size of the roughness elements.

8. NOMENCLATURE

D - Pipe Diameter, m

D_{cf} - Constricted pipe diameter, m

r_o - Pipe radius, m

r - Stream radius, m

$r(t)$ - Displacement frontal radius, m

$l(t)$ - Position of displacement front, m

$l_{\max}$ - Maximum displacement frontal position, m

y - Distance from the pipe wall, m

t - Time of displacement, s

C - A parameter accounting for local turbulence

n - Exponent

Q - Volumetric flow rate, m^3/s

$u(r)$ - Flow velocity, m/s

u_m - Mean velocity, m/s

$u_{\max}$ - Maximum velocity, m/s

$\bar{u}$ - Time average velocity, m/s

u' - Fluctuating velocity component, m/s

$\bar{u}_{\max}$ - Centreline velocity of a turbulent flow, m/s

u_{local} - Local velocity (Near wall velocity), m/s

v_* - Frictional velocity, m/s

u_{cf} - Constricted mean velocity, m/s

f - Friction factor

f_{cf} - Constricted friction factor

$\frac{dp}{dx}$ - Pressure gradient, Pa/m

$\frac{d\bar{u}}{dy}$ - Time average velocity gradient, s^{-1}

μ - Dynamic viscosity, Pas

υ_t - Turbulent kinematic viscosity

υ - Kinematic viscosity

τ - Shear stress, Pa

τ_l - Laminar shearing stress, Pa

τ_t - Turbulent shearing stress, Pa

9. REFERENCES

Andreopoulos, J., & Wood, D. H. (1981). The Response of a Turbulent Boundary Layer to a Short Length of Surface Roughness. *Journal of Fluid Mechanics , 118*, 143-164.

Carrasco-Teja, M., Frigaard, I. A., & Seymour, B. (2008). Cementing Horizontal Wells: Complete Zonal Isolation Without Casing Rotation. Calgary.

Ferizi, S. (2014). *Thesis Work: Cement Displacement Efficiency.* Trondheim: NTNU.

Greaves, F. C. (1963). Improved Primary Cementing Through Turbulent Flow Techniques. *Journal of Canadian Petroleum* , Edmonton, April 1963,40-44.

Herwig, H., Gloss, D., & Wenterodt, T. (2010). Flow in Channels With Rough Walls-Old and New Concepts. *Heat Transfer Engineering , 31:8*, 658-665.

Huang, K., Wan, J. W., Chen, C. X., Li, Y. Q., Mao, D. F., & Zhang, M. Y. (2013). Experimental Investigation on Friction Factor in Pipes with Large Roughness. *Experimental Thermal and Fluid Science , 50*, 147-153.

Huang, K., Wan, J. W., Chen, C. X., Mao, D. F., & Li, Y. Q. (2012). Experiments investigation of the effects of surface roughness on laminar flow in macro tubes. *Experimental Thermal and Fluid Science , 45*, 243-248.

Janna, W. S. (2010). *Introduction to Fluid Mechanics* (Fourth ed.). Boca Raton: CRC Press-Taylor & Francis Group.

Kandlikar, S. G. (2008). Exploring Roughness Effect on Laminar Internal Flow-Are We Ready for Change? *Nanoscale and Microscale Thermophysical Engineering , 12*, 61-82.

Keirsbulck, L., Labraga, L., Mazouz, A., & Tournier, C. (2002). Surface Roughness Effects on Turbulent Boundary Layer. *Journal of Fluids Engineering , 124*, 127-135.

Kundu, P. K., & Cohen, I. M. (2002). *Fluid Mechanics* (Second Edition ed.). San Diego, California: Elsevier Science.

Levi, E. (1978). Eddy Production Inside Wall Layers. *Journal of Hydraulic Research , 16:2*, 107-122.

Munson, B. R., Young, D. F., Okiishi, T. H., & Huebsch, W. W. (2009). *Fundamentals of Fluid Mechanics* (Sixth ed.). John Wiley & Sons.

Nakayama, Y., & Boucher, R. F. (1999). *Introduction to Fluid Mechanics.* Japan: Yokendo Co. LTD.

Nelson, E. B., 1990. Well Cementing. Texas: Schlumberger Educational Services.

Pope, S. B. (2000). *Turbulent Flows* (2nd ed.). New York: Cambridge University Press.

Rahman, M. (2011). *Mechanics of Real Fluids.* Southampton: WIT Press.

Reed, T. D., & Pilehvari, A. A. (1993). A New Model for Laminar, Transitional and Turbulent Flow of Drilling Muds. Oklahoma City: SPE.

Renpu, W., 2011. Advanced Well Completion Engineering. New York: Gulf Professional Publishing.

Silva, M. G., Martins, A. L., Barbosa, B. C., & Garcia, H. (1996). Designing Fluid Velocity Profiles for Optimal Primary Cementing. Port-of-Spain: SPE.

Skalle, P. (2002). Cementing Problems when Setting Casing Through Porous Gas & Water Bearing Formations. *OIL GAS European Magazine* .

Skalle, P., & Jafariesfad, N. (2014). Cement Displacement Efficiency in Smooth and Rough Pipes. Trondheim.

Smith, T. R. (1990, May). Cementing Displacement Practices-Field Applications. Society of Petroleum Engineers.

Taylor, J. B., Carrano, A. L., & Kandlikar, S. G. (2006). Characterization of the effect of surface roughness and texture on fluid flow—past, present, and future. *International Journal of Thermal Sciences , 45*, 962-968.

White, F. M. (2008). *Fluid Mechanics* (Seventh ed.). New York: McGraw-Hill.

Yang, S.-Q., Han, Y., & Dharmasiri, N. (2011). Flow Resistance Over Fixed Roughness Elements. *Journal of Hydraulic Research , 49:2*, 257-262.

10. APPENDICES

Appendix A.

Table 6: Simulation values of velocity from the center of the pipe of radius 0.005m to the wall at a constant flow rate of 0.000007065m³/s.

$C \rightarrow$	0	0.1	0.2	0.3	0.4	0.5	1
Radius, r[m]↓	Velocity, $u(r)$ [m/s]						
0	0.18	0.18	0.18	0.18	0.18	0.18	0.18
0.00001	0.17999928	0.17999928	0.17999928	0.17999928	0.17999928	0.17999928	0.17999928
0.00002	0.17999712	0.17999712	0.17999712	0.17999712	0.17999712	0.17999712	0.17999712
0.00003	0.17999352	0.17999352	0.17999352	0.17999352	0.17999352	0.17999352	0.17999352
0.00004	0.17998848	0.17998848	0.17998848	0.17998848	0.17998848	0.17998848	0.17998848
0.00005	0.17998200	0.17998200	0.17998200	0.17998200	0.17998200	0.17998200	0.17998200
0.00006	0.17997408	0.17997408	0.17997408	0.17997408	0.17997408	0.17997408	0.17997408
0.00007	0.17996472	0.17996472	0.17996472	0.17996472	0.17996472	0.17996472	0.17996472
0.00008	0.17995392	0.17995392	0.17995392	0.17995392	0.17995392	0.17995392	0.17995392
0.00009	0.17994168	0.17994168	0.17994168	0.17994168	0.17994168	0.17994168	0.17994168
0.00010	0.17992800	0.17992800	0.17992800	0.17992800	0.17992800	0.17992800	0.17992800
0.00011	0.17991288	0.17991288	0.17991288	0.17991288	0.17991288	0.17991288	0.17991288
0.00012	0.17989632	0.17989632	0.17989632	0.17989632	0.17989632	0.17989632	0.17989632
0.00013	0.17987832	0.17987832	0.17987832	0.17987832	0.17987832	0.17987832	0.17987832
0.00014	0.17985888	0.17985888	0.17985888	0.17985888	0.17985888	0.17985888	0.17985888
0.00015	0.17983800	0.17983800	0.17983800	0.17983800	0.17983800	0.17983800	0.17983800
0.00016	0.17981568	0.17981568	0.17981568	0.17981568	0.17981568	0.17981568	0.17981568
0.00017	0.17979192	0.17979192	0.17979192	0.17979192	0.17979192	0.17979192	0.17979192
0.00018	0.17976672	0.17976672	0.17976672	0.17976672	0.17976672	0.17976672	0.17976672
0.00019	0.17974008	0.17974008	0.17974008	0.17974008	0.17974008	0.17974008	0.17974008
0.00020	0.17971200	0.17971200	0.17971200	0.17971200	0.17971200	0.17971200	0.17971200
0.00021	0.17968248	0.17968248	0.17968248	0.17968248	0.17968248	0.17968248	0.17968248
0.00022	0.17965152	0.17965152	0.17965152	0.17965152	0.17965152	0.17965152	0.17965152
0.00023	0.17961912	0.17961912	0.17961912	0.17961912	0.17961912	0.17961912	0.17961912
0.00024	0.17958528	0.17958528	0.17958528	0.17958528	0.17958528	0.17958528	0.17958528
0.00025	0.17955000	0.17955000	0.17955000	0.17955000	0.17955000	0.17955000	0.17955000
0.00026	0.17951328	0.17951328	0.17951328	0.17951328	0.17951328	0.17951328	0.17951328

Appendix B.

Experimental data obtained by Ferizi (2014) through her laboratory work. The data are sorted to only take up to at most the Reynolds number value of 1800.

B1. Laboratory Measurements of Water displacing Oil in Slick Pipe

Displaced Volume [Litre]	Flow Rate, q [m³/s]	Reynolds Number, NRe	Percentage Oil Displaced [%]	Displaced Units
0.36	0.000005	645	72	0.76
2.28	0.000006	828	88	4.85
0.47	0.000006	854	64	1
0.38	0.000006	901	40	0.8
8.15	0.000007	1009	100	17.3
0.75	0.000007	1038	64	1060
0.34	0.000007	1054	68	0.72
1.34	0.000007	1065	80	2.84
6.24	0.000008	1162	92	13.25
1.3	0.000008	1188	84	2.76
4.09	0.000009	1233	80	8.69
1.89	0.000009	1258	32	4
1.23	0.000009	1276	80	2.6
1.89	0.000009	1285	52	4

1.26	0.00001	1461	76	2.68
2.68	0.000011	1516	72	5.69
0.23	0.000011	1522	24	0.48
4.07	0.000011	1629	88	8.65
2.45	0.000011	1642	80	5.21
6.32	0.000012	1685	96	13.41
1.21	0.000012	1747	76	2.56

B2. Medium Rough pipe, Water Displacement

Displaced Volume [m^3]	**Flow Rate, q [m^3/s]**	**Reynolds Number, NRe**	**Percentage Oil Displaced [%]**	**Displaced Units**
0.00034	0.000001	162	72	0.72
0.00047	0.000003	384	100	1
0.00047	0.000003	392	100	1
0.00157	0.000003	398	100	3.32
0.0003	0.000005	729	64	0.64
0.00066	0.000006	832	100	1.4
0.00128	0.000009	1353	92	2.72
0.00034	0.00001	1475	72	0.72
0.00811	0.000011	1613	100	17.22
0.00828	0.000011	1632	100	1758
0.00615	0.000012	1678	100	13.05
0.00415	0.000012	1732	96	8.81
0.00119	0.000012	1736	96	2.52

0.0003	0.000012	1761	60	0.64

B3. **Tests When the Pipe was not Re-filled after every attempt**

Displaced Volume [m^3]	**Flow Rate, q [m^3/s]**	**Reynolds Number, NRe**	**Percentage Oil Displaced [%]**	**Displaced Units**
0.00038	0.000008	1077	12	0.8
0.00113	0.000008	1179	76	2.4
0.00123	0.000009	1277	76	2.6
0.00264	0.000009	1317	80	5.61
0.00815	0.000009	1337	92	17.3
0.00047	0.000009	1346	72	1
0.00396	0.00001	1400	84	8.41
0.00566	0.00001	1405	84	12.01
0.00811	0.00001	1410	92	17.22
0.00283	0.00001	1411	84	6.01
0.00815	0.00001	1451	100	17.3
0.00405	0.00001	1455	84	8.61
0.00604	0.00001	1487	84	12.81
0.0057	0.000011	1561	96	12.09
0.00402	0.000012	1670	92	8.53
0.00283	0.000012	1760	88	6.01

B4. **Very Rough, Water Displacement**

Displaced Volume [m^3]	Flow Rate, q [m^3/s]	Reynolds Number, NRe	Volume of Oil [m^3]	Percentage Oil Displaced [%]	Number of Displaced Volumes
0.00052	0.000001	76	0.00039	82	1.1
0.00026	0.000001	160	0.00026	56	0.56
0.00023	0.000001	194	0.00023	48	0.48
0.00147	0.000003	375	0.00047	100	3.12
0.00066	0.000003	439	0.00045	96	1.4

B5. Slick pipe, Viscous Displacement

Displaced Volume [m^3]	Flow Rate, q [m^3/s]	Reynolds Number, NRe	Percentage Oil Displaced [%]	Number of Displaced Volumes
0.00043	0.000001	31	84	0.92
0.00415	0.000003	78	96	8.81
0.00245	0.000003	87	52	5.21
0.00147	0.000004	92	84	3.12
0.00102	0.000005	128	92	2.16
0.00117	0.000007	181	88	2.48
0.0066	0.000012	294	100	14.01
0.00085	0.000027	698	64	1.8
0.00249	0.000029	746	100	5.29

B6. **Medium Rough Pipe, Viscous Displacement**

Displaced Volume [m^3]	**Flow Rate, q [m^3/s]**	**Reynolds Number, NRe**	**Percentage Oil Displaced [%]**	**Number of Displaced Volumes**
0.00123	0.000005	691	100	2.6
0.00245	0.000008	1080	100	5.2
0.00449	0.000009	1286	100	9.5
0.00047	0.000015	2177	100	1
0.00047	0.000026	3749	92	1
0.00132	0.000029	4199	96	2.8

B7. Very Rough Pipe, Viscous Displacement

Displaced Volume [m^3]	**Flow Rate, q [m^3/s]**	**Reynolds Number, Nre**	**Percentage Oil Displaced [%]**	**Number of Displaced Volumes**
0.00434	0.000007	1025	100	9.2
0.00255	0.000009	1274	100	5.4
0.00622	0.000009	1350	100	13.2
0.0082	0.000011	1631	100	17.4
0.00141	0.000013	1875	100	3
0.00049	0.000016	2264	100	1

Appendix C.

Table 7: Simulation data obtained from the adjusted theoretical model.

C →	1	1.1	1.4	1.5	1.6	1.9	2
Radius, r[m] ↓	U (r) [m/s]						
0	0.4076	0.4484	0.5707	0.6115	0.6522	0.7745	0.8153
0.0001	0.4075	0.4482	0.5705	0.6113	0.6521	0.7744	0.8151
0.0002	0.4070	0.4478	0.5700	0.6108	0.6516	0.7739	0.8146
0.0003	0.4062	0.4469	0.5692	0.6100	0.6508	0.7731	0.8138
0.0004	0.4050	0.4458	0.5681	0.6089	0.6496	0.7719	0.8127
0.0005	0.4036	0.4443	0.5666	0.6074	0.6482	0.7704	0.8112
0.0006	0.4018	0.4425	0.5648	0.6056	0.6464	0.7687	0.8094
0.0007	0.3997	0.4404	0.5627	0.6035	0.6442	0.7665	0.8073
0.0008	0.3972	0.4380	0.5603	0.6010	0.6418	0.7641	0.8049
0.0009	0.3944	0.4352	0.5575	0.5983	0.6390	0.7613	0.8021
0.001	0.3913	0.4321	0.5544	0.5952	0.6359	0.7582	0.7990
0.0011	0.3879	0.4287	0.5510	0.5917	0.6325	0.7548	0.7956
0.0012	0.3842	0.4249	0.5472	0.5880	0.6287	0.7510	0.7918
0.0013	0.3801	0.4209	0.5431	0.5839	0.6247	0.7470	0.7877
0.0014	0.3757	0.4164	0.5387	0.5795	0.6203	0.7426	0.7833
0.0015	0.3710	0.4117	0.5340	0.5748	0.6155	0.7378	0.7786
0.0016	0.3659	0.4067	0.5290	0.5697	0.6105	0.7328	0.7735
0.0017	0.3605	0.4013	0.5236	0.5643	0.6051	0.7274	0.7682
0.0018	0.3548	0.3956	0.5179	0.5586	0.5994	0.7217	0.7625
0.0019	0.3488	0.3895	0.5118	0.5526	0.5934	0.7157	0.7564
0.002	0.3424	0.3832	0.5055	0.5462	0.5870	0.7093	0.7501
0.0021	0.3357	0.3765	0.4988	0.5396	0.5803	0.7026	0.7434
0.0022	0.3287	0.3695	0.4918	0.5325	0.5733	0.6956	0.7364
0.0023	0.3214	0.3622	0.4844	0.5252	0.5660	0.6883	0.7290
0.0024	0.3137	0.3545	0.4768	0.5175	0.5583	0.6806	0.7214
0.0025	0.3057	0.3465	0.4688	0.5096	0.5503	0.6726	0.7134
0.0026	0.2974	0.3382	0.4605	0.5012	0.5420	0.6643	0.7051
0.0027	0.2888	0.3295	0.4518	0.4926	0.5334	0.6557	0.6964
0.0028	0.2798	0.3206	0.4429	0.4836	0.5244	0.6467	0.6874
0.0029	0.2705	0.3113	0.4336	0.4743	0.5151	0.6374	0.6782

0.003	0.2609	0.3017	0.4239	0.4647	0.5055	0.6278	0.6685
0.0031	0.2509	0.2917	0.4140	0.4548	0.4955	0.6178	0.6586
0.0032	0.2407	0.2814	0.4037	0.4445	0.4853	0.6076	0.6483
0.0033	0.2301	0.2708	0.3931	0.4339	0.4747	0.5970	0.6377
0.0034	0.2191	0.2599	0.3822	0.4230	0.4637	0.5860	0.6268
0.0035	0.2079	0.2487	0.3710	0.4117	0.4525	0.5748	0.6155
0.0036	0.1963	0.2371	0.3594	0.4001	0.4409	0.5632	0.6040
0.0037	0.1844	0.2252	0.3475	0.3882	0.4290	0.5513	0.5921
0.0038	0.1722	0.2130	0.3352	0.3760	0.4168	0.5391	0.5798
0.0039	0.1596	0.2004	0.3227	0.3635	0.4042	0.5265	0.5673
0.004	0.1468	0.1875	0.3098	0.3506	0.3913	0.5136	0.5544
0.0041	0.1335	0.1743	0.2966	0.3374	0.3781	0.5004	0.5412
0.0042	0.1200	0.1608	0.2831	0.3238	0.3646	0.4869	0.5277
0.0043	0.1062	0.1469	0.2692	0.3100	0.3507	0.4730	0.5138
0.0044	0.0920	0.1327	0.2550	0.2958	0.3366	0.4588	0.4996
0.0045	0.0775	0.1182	0.2405	0.2813	0.3220	0.4443	0.4851
0.0046	0.0626	0.1034	0.2257	0.2664	0.3072	0.4295	0.4703
0.0047	0.0474	0.0882	0.2105	0.2513	0.2920	0.4143	0.4551
0.0048	0.0320	0.0727	0.1950	0.2358	0.2765	0.3988	0.4396
0.0049	0.0161	0.0569	0.1792	0.2200	0.2607	0.3830	0.4238
0.005	0.0000	0.0408	0.1631	0.2038	0.2446	0.3669	0.4076